Hot Nanoparticles

Jollans, T.G.W.

4 On picosecond-to-nanosecond heat transfer around a gold nanoparticle

We use pump-probe extinction spectroscopy to study the cooling dynamics of a single gold nanoparticle with picosecond time resolution. By continuously heating the nanoparticle, we can measure how nanoscale picosecond heat transfer dynamics from the particle to its environment change with temperature. We discuss the constraints laser-induced damage to the nanoparticle and its environment place on the measurement technique and contemplate picosecond control and investigation of vapour nanobubble formation.

4.1 Introduction

Heat transfer and boiling processes have been extensively studied at space and time scales most relevant to industrial processes, such as the cooling of apparatus ranging from hand-held devices to nuclear power plants. They have further been studied scientifically at all edges of that range, including at (tens of) nanometer size and (tens of) nanosecond time scales in chapter 2 of this thesis.

Measurements of heat transfer on *pico*second timescales have been reported e.g. for bulk metals [93], thin films [94, 95], and metallic nanoparticles [96, 97]. At small sizes in particular, the universally optical picosecond-time measurements involving heat transfer have, however, frequently been characterized by melting and laser ablation of the studied materials [23, 44, 98, 99], be it intentionally or not.

Many studies of heat transfer at picosecond time and nanometer size scales have focussed on heat transfer in metals, where processes are often fast and optical studies are feasible. Heat transfer involving metals, however, is a broad church and includes heat transfer from metals to their non-metal surroundings. In particular, cooling of metal nanoparticles, heated by a picosecond or femtosecond laser pulse, passing heat to their surroundings, has been studied thoroughly in the case where the nanoparticles are in equilibrium with their surroundings before the arrival of the laser pulse [97].

The extreme case of this problem — the absorption of a lot of energy in a short amount of time by a nanoparticle under pulsed illumination — can (besides ablation in one form or another) result in the formation of vapour nanobubbles, that is to say rapid boiling in the environment due to the large amount of deposited heat.

There have been some time-resolved studies of pulse-excited plasmonic vapour nanobubble dynamics based on pump-probe techniques, e.g. by Plech and co-workers using small-angle X-ray scattering (SAXS) and transient optical extinction [42, 100], and by Katayama et al. [101] using spectrally resolved transient optical extinction. The time resolution of these ensemble studies has been, however, limited to the tens of ps, all while they indicate that the dynamics of the earliest stages of nanobubble formation may well be faster. The dynamics of nanobubble formation *per se* thus appear to be obscured.

As Katayama et al. [101] point out, since their results are ensemble-averaged, the time resolution they can achieve is limited by the dynamical heterogeneity

from nanoparticle to nanoparticle. To go down to the single picosecond, we must therefore (as, indeed, they point out) go to a single-particle experiment.

As we will be performing a stroboscopic pump-probe technique to achieve picosecond time resolution (see § 4.2.1), even without particle-to-particle differences, we may still be limited by dynamical heterogeneity: as the measurement requires integration over many millions of consecutive laser pulses (and thus boiling events), any variation of the behaviour from pulse to pulse will limit the experiment's resolution and fidelity.

There are several possible sources of pulse-to-pulse variation: Firstly, there may be a slow build-up of heat in the nanoparticle as the laser pulses arrive in rapid succession during the measurement. For each and every event to be equivalent to the last, the laser pulse fluences must be chosen to be low enough that the particle can dissipate all the heat it has absorbed before the next laser pulses arrive[1].

If the particle gets hot enough, it might melt, or, at least, there may be some degree of surface melting [102]. In and of itself, this may not be an issue — as long as the sample remains stable. The nanoparticle must not, however, reshape, shrink, shatter, drill into the substrate, or otherwise change [23, 103, 104] over the course of the experiment.

Further, if initial vapour nanobubble formation is limited by a process with some degree of randomness (such as diffusion), this may translate to a random 'speed' (for want of a better word) of boiling and bubble formation. After all, Hou et al. [41] found a random component in vapour nanobubble formation under continuous heating, which can also be seen in chapter 2 of this thesis, particularly fig. 2.3–II.

4.2 Method

4.2.1 Premise

We perform a transient optical extinction measurement in a pump-probe configuration. This means that we prepare two laser pulse streams, with a delay τ between the two pulse streams. Each time the first pulse, named the 'pump', reaches the sample, a single gold nanoparticle, it excites it, depositing

[1] There is no requirement for the particle to return to room temperature, it must merely be able to reach a stable equilibrium in which each event is indistinguishable from the last.

a certain amount of energy within. This kick-starts a process in which this additional energy escapes the particle in one way or another, primarily as heat. A delay τ later, the second pulse, dubbed 'probe', arrives and interacts with the sample as it is at the instant a delay τ after the sample was excited.

This is a well-known stroboscopic technique: because the probe laser is pulsed, we only get information about the state of the sample during the brief moments during the pulse. At each and every one of these moments, a pump pulse had arrived a time τ beforehand. The transmission of the probe beam by the sample then corresponds, in this configuration, to the transmission a time τ after excitation, and can easily be integrated over experimentally feasible time scales. If we now vary τ, we build up, point by point, a reconstructed time trace, or, a spectrum of the (mean) transmission as a function of time. The temporal resolution is limited in principle by the pulse widths of the two lasers.

So far for the 'traditional' technique — in an attempt to limit the sources of dynamical heterogeneity raised above, we introduce an additional, in this case continuous-wave, laser to the experiment. We use it to move away from what we might call 'extreme pulsed heating', and somewhat close to the experiment of chapter 2 and ref. [41]. The CW laser is used to heat the nanoparticle (and environs) to the point where it is nearly, but not quite, ready to explosively form a vapour nanobubble. In the language of § 2.3.1, we aim to hold the particle just below the boundary between régimes I and II.

With the particle so pre-heated, we hope (vainly, perhaps) to reduce any delay between the absorption of the pump pulse, the sudden kick across the threshold into boiling régime II, as it were, and the actual formation of the vapour nanobubble. This also reduces the amount of heat we need to supply in each laser pulse, as well as the maximum temperature within the particle, which may reduce the risk of damage to the sample.

4.2.2 Gold nanoparticle excited by a laser pulse

From the gold nanoparticle absorbing a laser pulse to the absorbed energy having been fully dissipated, a number of processes occur at well-separated time scales:

First of all, the laser-excited electrons thermalize with the remaining electron population on a time scale on the order of 10 fs [22]. In our case, the laser pulses have a pulse length on the order of hundreds of fs, meaning this process

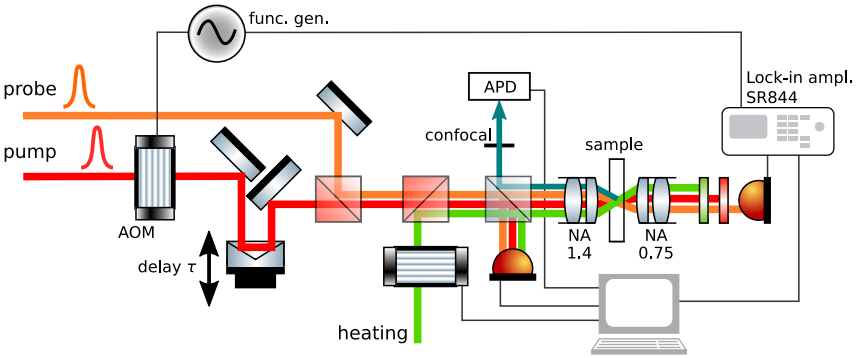

Figure 4.1: Sketch of the main components of the experimental setup. The time-resolved extinction measurement comes from a fast photodetector (right) via the lock-in amplifier.

happens while the energy is being absorbed and is too fast to detect. The electrons reach temperatures on the order of 10^3 K (see chapter 5), which shifts and broadens the plasmon resonance, and is therefore visible. Secondly, heat is transferred from the hot electrons to the metal lattice on a timescale of some picoseconds [105] .

Thirdly, heat is transferred out into the medium and diffuses outwards into the bath. This typically occurs on a timescale on the order of hundreds of picoseconds. At the same time, the sudden heating of the nanoparticle launches it into a mechanical breathing mode. The period of these oscillations depends on the size of the nanoparticle and is on the order of ~10 ps. They are among the most striking features of the time traces shown in this chapter, and have been studied extensively in the past [106, 107], but for the purposes of this chapter they are incidental to the measurement technique and will not be discussed in any detail.

4.2.3 Experimental details

Three laser beams are tightly focussed on a single 80 nm gold nanoparticle. Two of them are synchronized sub-ps pulsed lasers with a repetition rate of 75.8 MHz: a titanium sapphire in the near infrared (λ = 785 nm), which will excite the nanoparticle, pumps a frequency-doubled optical parametric oscillator (~600 nm), used to probe the system. The delay τ from one pulse to

the other is varied using a mechanical delay line with a length of 1 ns, and is defined such that a positive delay $\tau > 0$ corresponds to the visible probe pulse arriving after the pump pulse.

A scheme of the experimental setup is shown in fig. 4.1; we measure the light from the probe beam that is transmitted through the sample using a fast photodetector (FEMTO Messtechnik), which is equivalent to measuring the extinction of the beam[2]. To make small changes in an already weak signal from a single nanoparticle measurable, we use a lock-in detection mode.[3] The intensity of the pump laser beam is modulated with an acousto-optic modulator (AOM) at ~1 MHz, which allows a lock-in amplifier (Stanford Research Systems SR844) to extract the effect of the pump pulse on the extinction measurement by locking in on the modulation frequency.

The integration time of the lock-in amplifier is set to 30 ms. Meanwhile, the delay line is slowly moving, covering 0.25 ps every 30 ms (corresponding to 1.25 mm s^{-1}). The output of the amplifier is recorded every 60 ms, which produces an ultrafast time trace (a.k.a. a pump-probe spectrum) of the response to excitation by the pump pulse with a resolution of 0.5 ps, where every datapoint corresponds to 4.5 million laser pulses.

The third laser beam, a continuous-wave laser with a wavelength of 532 nm, is used to pre-heat the nanoparticle. Its intensity is controlled with a second AOM and is kept stable throughout the acquisition of each spectrum.

The nanoparticles are deposited on a cover slip, either borosilicate glass (Menzel) or fused silica, and the cover slip is attached to a PDMS cell holding a reservoir of water. The nanoparticles are thus attached on one side to glass, and otherwise surrounded by water. In the case of borosilicate glass, the cell is a flow cell attached to tubes whose ends are some 15 cm from the nanoparticle. In the case of the fused silica substrate, the cell is sealed. In either case, the depth of the reservoir (perpendicular to the substrate) is on the order of ~100 µm, and the extent parallel to the substrate is several millimetres (or, along one direction of the flow cell, centimetres). More succinctly, the reservoir is very large compared to the nanoparticle.

In order to move the particles into the focus of the microscope, the sample is mounted on a piezoelectric 3D nanopositioning system (Physik Instrumente).

[2] Nota bene, both scattering and absorption contribute significantly to the extinction.

[3] An alternative strategy would be to integrate for a very long time, which is the approach used in chapter 5.

4.2.4 Measurement protocol

The measurements presented herein were performed following the same basic protocol: After ensuring that the experimental setup is well-adjusted, a single nanoparticle with the expected behaviour (without additional heating) is selected. A series of pump-probe time traces with different CW heating intensities are then recorded:

First, we ensure the particle is in focus by scanning the focus across 1 µm along each of the Cartesian axes and optimizing the CW-excited photoluminescence at low intensity. Then, the AOM in the CW heating beam path is set to switch to a target heating power. The heating power is measured before the objective. The shutters blocking the pulsed laser beams are then opened, and a pump-probe time trace is acquired by scanning the delay line from slightly negative delay (probe arrives before pump) to positive delay (pump arrives before probe). Once the time trace has been acquired, the process is repeated.

We start at low heating and move to higher heating power step by step. In order to distinguish reproducible behaviour from irreversible changes to the nanoparticle, we alternate between acquisitions without CW heating and acquisitions with non-zero CW heating: each heated measurement is preceded and succeeded by one without heating. All measurements without CW heating should give the same result; if they do not, we know that there has been some irreversible change to the sample (e.g. damage to the nanoparticle or its surroundings).

4.3 Results

4.3.1 Preliminary measurements on borosilicate glass

Fig. 4.2a shows the measurements as they were meant to be, with the required consistency for measurements at zero heating. The time traces show the documented features: an initial spike lasting a few picoseconds at $\tau = 0$. This is due to the high initial temperature of the conduction electrons. After those first few picoseconds, we see a slow decay of the excitation into the environment, and the breathing mode oscillations of the particle. The decay constant of heat transfer from the particle into the environment appears to be slightly altered for the heated particle.

If we heat the same particle more (fig. 4.2b), however, we begin to see telltale

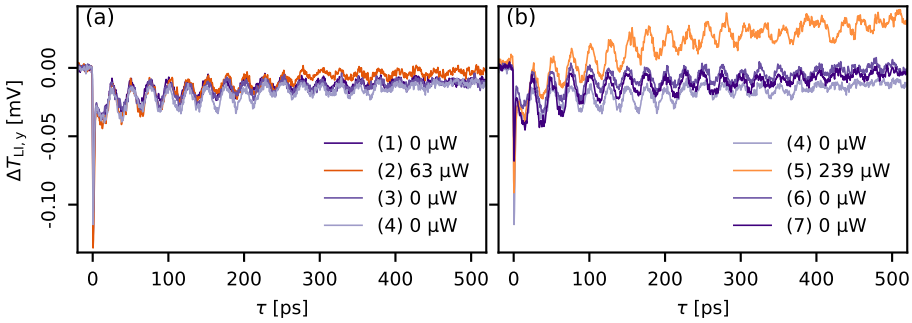

Figure 4.2: Example time traces on borosilicate glass for one nanoparticle, split across two panels for clarity. Numbers (*n*) indicate the order in which they were measured. Powers are CW heating powers in the back focal plane. **(a)** Three traces at zero heating, before and after non-zero heating, which are, as intended, identical. The trace with non-zero heating shows a slight shift. **(b)** A higher heating intensity time trace shows a markedly different result; the zero-heating time traces before and after are inconsistent with each other, indicating possible damage to the nanoparticle.

signs of damage to the particle: a measurement with zero additional heating after the fact (traces (6) and (7)) is inconsistent with a measurement ante hoc (trace (4)). Since the acquisition of a such a time trace takes a finite amount of time during which the particle may change, we cannot tell, from looking at a measurement such as trace (5) in fig. 4.2b, which parts of it are due to the change in pulse-to-pulse delay τ, and which are due to slow changes to the particle *unless* we know with some degree of certainty that the particle has not, in fact, changed.

In the example in fig. 4.2b, the irreversible change to the particle appears to be slight, and the 'hot' trace (5) in particular bears some resemblance to the measurements presented as probable nanobubble time traces in Lei Hou's thesis [108]. However, not only has the particle already changed slowly, but, in subsequent measurements (at higher heating), its pump-probe behaviour changes very dramatically, as seen in fig. 4.3a.

A major contributing factor to the contrast of these time traces is the plasmon resonance shifting, slightly, due to the excitation. It stands to reason that the sign of this change corresponds to the slope of the spectrum at our probe

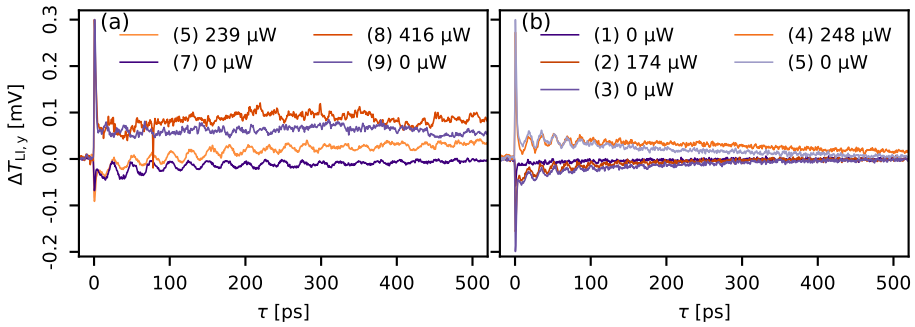

Figure 4.3: Examples of a drastic change in behaviour after heated pump-probe time traces. **(a)** Measurements of the same particle as fig. 4.2; two traces are shown both here and in fig. 4.2b for comparison. **(b)** Example of similar behaviour on a different particle.

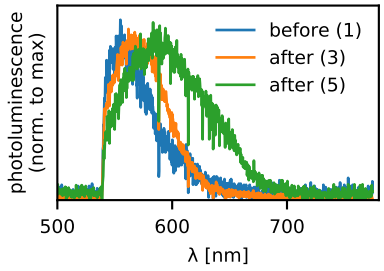

Figure 4.4: Photoluminescence spectra (excited at 532 nm) of the particle from fig. 4.3b at the start of the measurement, and after two subsequent heated time-trace acquisitions, showing a significant shift in the PL peak.

wavelength $\partial/\partial\lambda[\sigma_{\text{sca}}(\lambda_{\text{probe}})]$. The change in sign seen in 4.3a and for many other particles, e.g. in fig 4.3b, is therefore likely to correspond to a shift in the plasmon resonance from one side of the probe wavelength to the other.

Indeed, photoluminescence spectra, shown in fig. 4.4, evidence such a shift. After subsequent CW-heated pump-probe measurements, the resonance seen in the photoluminescence spectrum shifts to the red step by step. This may be due to an elongation of the initially spherical nanoparticle, or, more probably, due to localized ablation of the glass substrate [104].

In all our measurements on borosilicate glass, any significant change in the time traces was accompanied by such irreversible changes to the behaviour.

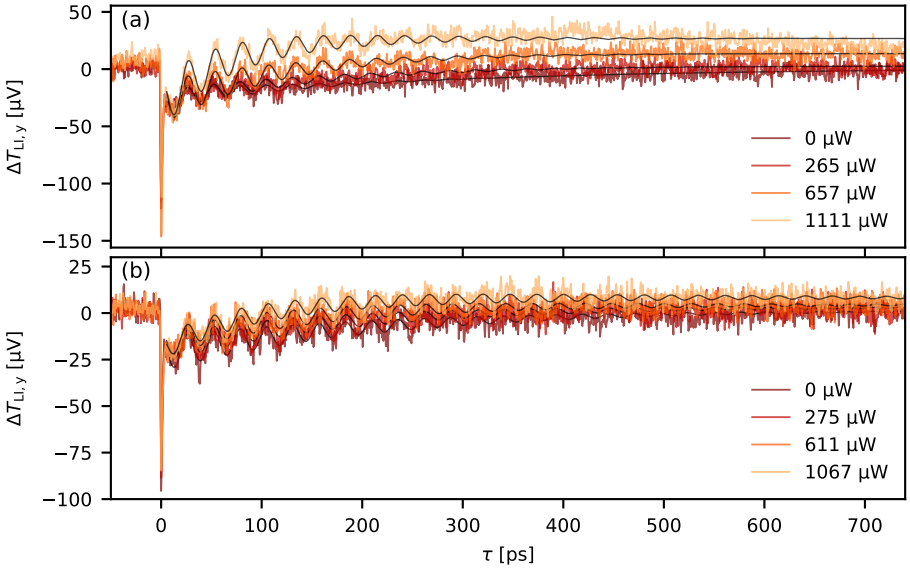

Figure 4.5: Selected time traces at different heating powers of two gold nanoparticles [**(a)** one, **(b)** the other] on a fused silica substrate. Black lines are fits to eq. (4.1).

4.3.2 Fused silica substrate

At this point we turn to fused silica as an alternative substrate with a higher melting point, making it more stable in the face of high heating, and damage to the substrate around the nanoparticle less likely.

This does not eliminate concerns about damage to the nanoparticles, of course, but it gives us a larger window of heating powers which we can use before damage sets in. At sufficiently high heating powers, damage to the particle looks much the same as it did on the borosilicate substrate, but at lower heating powers, significant changes to the time traces could be observed:

Fig. 4.5 shows illustrative time traces for two nanoparticles on the fused silica substrate for which the time traces at different heating powers were quite reproducible, and where there does not appear to have been any significant damage.

At higher heating power, the excited signal appears to decay more rapidly, but then, in several cases (e.g. fig. 4.5a), crosses the $\Delta T = 0$ line and changes

sign to eventually decay to zero from the other side. Even when the signal does not change sign, what appears to be a faster decay rate is likely in fact caused by whatever effect causes traces with more pronounced effects to cross zero.

In order to parametrize the time traces without any regard for the physics of the processes at work, we use a simple function:

$$\Delta T_{\text{fit}}(\tau) \stackrel{!}{=} Ae^{-\alpha\tau} + Be^{-\beta\tau}\cos\left(2\pi\nu\tau + \varphi\right) + C. \tag{4.1}$$

Here, the parameters A and α describe the initial decay, C is the value the decay appears to approach, and B, β, ν and φ describe the particle's breathing mode oscillations and their decay. Note that this fit does not describe the decay back to zero from C which can be seen well in the highest-power trace of fig. 4.5a after some 500 ps.

The derived fit parameters for the measurement series the traces in fig. 4.5 are shown in fig. 4.6. We can look at the fit parameters both as a function of heating power, to determine how the behaviour of the particles depends on the heating, and also as a function of real experimental time elapsed. Doing the latter is important since we know there is a risk of the particle and substrate changing slowly over time.

Recall, at this point, that we alternate between heated and non-heated acquisitions in our measurements. Every heated time trace, and thus every point in the plots in 4.6 at $P_{\text{cw}} \neq 0$ is preceded and succeeded by ones at $P_{\text{cw}} = 0$. Furthermore, we move from low heating power to high heating power. Considering this measurement protocol allows us to interpret the plots of the fit parameters as a function of experimental macro-time:

If a parameter does not depend on heating power, and does not drift over time, it will remain constant to within the experimental noise envelope over the entire plot. This is the behaviour of φ. If a parameter does depend on heating power, but does not drift independently over time, the macro-time plot should be split into two branches: one branch, the 'heated' branch, will change over time (with the heating power); the other, the $P_{\text{cw}} = 0$ branch, will remain constant. The plots for A, α and C are examples of this behaviour. If a parameter drifts independently over time reflecting some irreversible change to the nanoparticle, the plot will reflect this drift. The plot for B in 4.6a shows this behaviour clearly; both plots for ν show it somewhat less clearly.

The three parameters that we would expect to describe heat transfer from

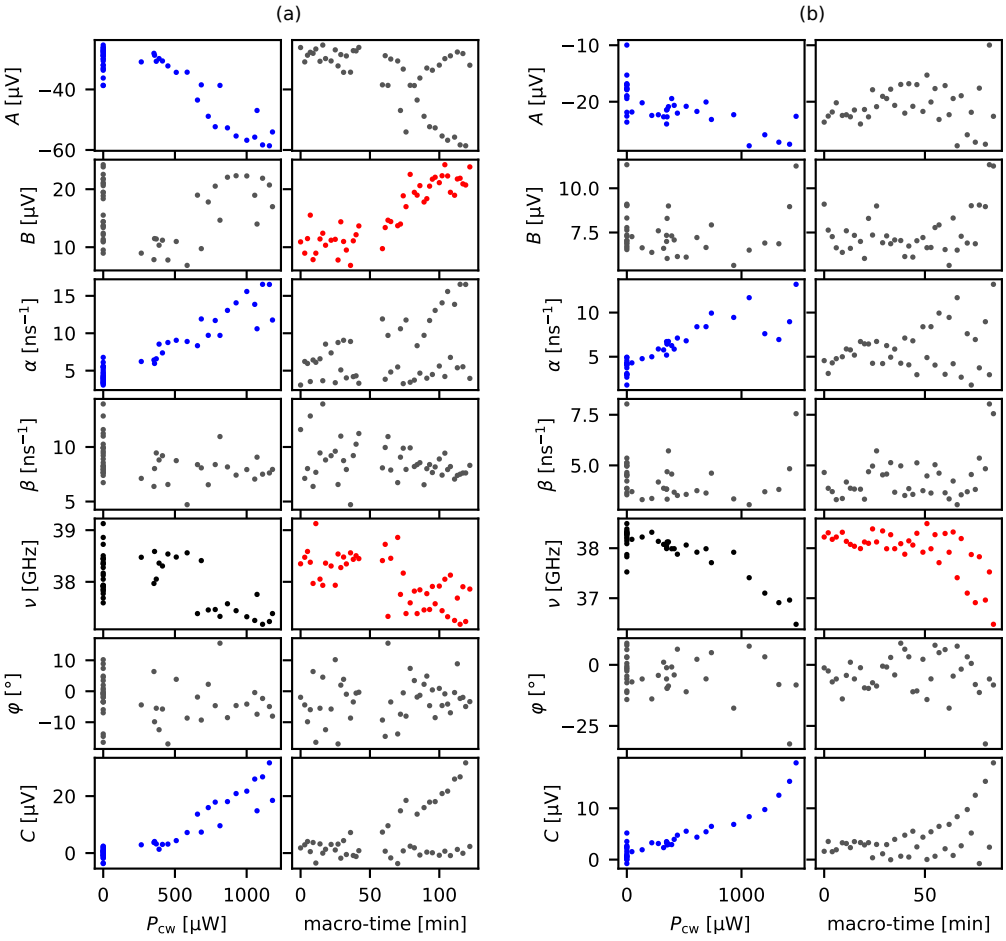

Figure 4.6: All fit parameters according to eq. (4.1) of all time traces of the particles from fig. 4.5, as a function of both CW heating power (left columns) and wall time from the first measurement of the series (right columns). Blue dots indicate parameters that appear to depend reproducibly on heating power. Red dots indicate parameters that show evidence of irreversible change over the course of the experiment. Grey dots permit no conclusion; ν (black dots) appears to show both a reproducible shift as a function of heating power and an irreversible change over time.

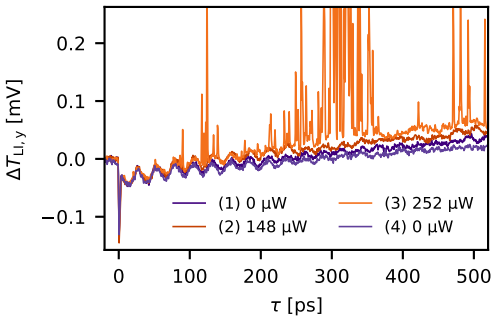

Figure 4.7: Representative example time traces in *n*-pentane, showing instability not observed in water.

the gold lattice into the environment in one way or another, A, α and C, then, do appear to depend reproducibly on the heating power. The oscillation frequency, ν, also appears to be reduced by higher heating power. This is an expected consequence of the change of the elastic moduli with temperature, and, since $\nu \propto R^{-1}$, of thermal expansion. However, ν also appears to drift over time.

These parameters appear to vary approximately linearly with heating power even as the nanoparticle is accumulating some degree of damage. There is no indication of a sharp nonlinear change in any of the parameters that may indicate the presence of a phase transition (such as bubble formation).

4.3.3 Other liquids

In order to encourage vapour nanobubble formation, we attempted the same experiment in other media with lower boiling points. In *methanol*, the time traces for practically all nanoparticles were inconsistent with each other to the point of absurdity, both on borosilicate glass and on fused silica. The inescapable and dramatic changes to the particle behaviour may be indicative of unintended (photo)chemical reactions.

In *pentane*, the time traces were generally more consistent, but any nanobubble formation that may have occurred was not synchronized with the laser pulses. Fig. 4.7 shows some example measurements in pentane; sudden spikes as seen in the highest-heating trace consistently appear at similar heating powers and are accompanied by no or little damage to the nanoparticle. They may correspond to spontaneous vapour bubble formation around the nanoparticle.

4.4 Discussion

We have measured picosecond extinction time traces of single gold nanoparticles under different CW heating conditions. At high heating, the change in extinction is observed to change sign before eventually decaying to zero.

It appears that two different contributions to the change in extinction with opposite signs are in competition with one another. At short times, one contribution dominates under all heating conditions, while at later times and high temperatures, the other contribution may become significant.

We can identify at least three subsystems whose temperature may affect the signal: the gold nanoparticle itself, the water it is surrounded by, and the fused silica substrate on which it sits. The temperatures of all three change, the refractive indices of all three depend on temperature, and the refractive indices (or: refractive index distributions) of all three will affect the signal.

At short times, before the absorbed heat has had time to diffuse into the surroundings, the signal is dominated by the change in the optical properties of gold. The 'starting point' at $\tau \approx 5\,\mathrm{ps}$ changes very little depending on the background CW heating power. Therefore, the properties of gold itself are unlikely to have much of an influence on the variation in the time traces.

At longer times, the temperature dependence of the refractive index distributions in the environment dominates the optical properties. At this point we can make note of the fact that the change of refractive index with temperature $\partial n/\partial T$ is negative for liquid water [109], but positive for fused silica [110].

We might imagine that the balance between the influence of the substrate and the influence of the medium shifts depending on the temperature. We know, in any case, that, for water,

$$\left(\frac{\partial n}{\partial T}\right)_p < 0 \qquad \text{and} \qquad \left(\frac{\partial n}{\partial T}\right)_V < 0$$

everywhere in the liquid phase so it does not appear that the measurements approaching zero from different sides can be due to the properties of the water alone.

4.5 Conclusion

We have measured dependence of picosecond time traces of the cooling dynamics of a heated single gold nanoparticle on the heating power. Surprisingly,

the sign with which the optical extinction approaches equilibrium depends on heating power. This may be linked to the different thermal properties and the different signs of $\partial n/\partial T$ of the liquid medium and the adjoining substrate.

For the parameter range in which the nanoparticle is stable (i.e. its behaviour does not change irreversibly), no sign of vapour bubbles consistently triggered by the pump pulses was observed. In cases where the nanoparticle is *not* stable, it is impossible to discriminate between ultrafast dynamics which occur with every laser pulse and slow changes which occur over the duration of the measurement. The preliminary measurements by Hou [108] may have been linked to such slow changes.

When using pentane rather than water, thus lowering the temperatures needed for vapour bubble generation, measurements showed violent instability (fig. 4.7) somewhat reminiscent of explosive bubble formation as seen in real-time measurements (e.g. fig. 2.3–II). This might be a signature of random bubble formation that is not triggered consistently by the pump laser pulse, or even not linked to the laser pulse(s) at all.

If this is the case, and if the bubbles form in response to random fluctuations in temperature and pressure, this might be remedied by better control of those variables. It appears unlikely that attempting to control temperature and pressure at a macroscopic scale would result in the required nanoscale stability, but vapour nanobubble generation in a well-controlled microchannel or microchamber may be worth exploring.

If, on the other hand, random bubble formation occurs in response to thermal (Brownian) fluctuations of the sort that are fundamentally unavoidable at high temperature, then the enterprise of picosecond control of nanoscale boiling may be doomed from the outset. The attempt in this chapter of using laser pulses as an artificial small fluctuation that would 'take precedence' (in a manner of speaking), in any case, has not proven fruitful.